Journal of Power Sources 232 (2013) 34–41

Contents lists available at SciVerse ScienceDirect

Journal of Power Sources

journal homepage: www.elsevier.com/locate/jpowsour

Direct utilization of fermentation products in an alcohol fuel cell

David M. Mackie [a], Sanchao Liu [a], Marcus Benyamin [a], Rahul Ganguli [b], James J. Sumner [a,*]

[a] U.S. Army Research Laboratory, Sensors and Electron Devices Directorate, Adelphi, MD 20783, USA
[b] Teledyne Scientific & Imaging, LLC, 1049 Caminos Dos Rios, Thousand Oaks, CA 91360, USA

HIGHLIGHTS

► Used fermented sugar in a passive DAFC; only solids >0.2 μm removed from fermentate.
► DAFC performance on fermentate can be comparable to that of aqueous ethanol.
► Ionic strength and ethanol concentration of the fermentate had the largest effects.

ARTICLE INFO

Article history:
Received 25 October 2012
Received in revised form
11 January 2013
Accepted 15 January 2013
Available online 22 January 2013

Keywords:
Proton exchange membrane fuel cell
Microbial
Ethanol
Yeast
Fermentation
Glucose

ABSTRACT

Due to energy demands and environmental concerns there has been a great interest in searching out renewable energy sources as an alternative to fossil hydrocarbons. These must also be environmentally sustainable and convenient to implement. Glucose has been proposed as a renewable energy source for several reasons including its energy density, safety, sustainability, and the ability to be scavenged from native ecosystems or from waste streams. Here we describe the use of a bio-hybrid fuel cell to oxidize the glucose to ethanol and limit parasitic power losses by using the fermented alcohol with minimal preparation in a direct alcohol fuel cell. Moving from using dilute alcohol in deionized water to the complex matrices of fermented media raises many questions about the performance and lifetime of the fuel cell and its components. These questions include but are not limited to the effects of starting materials and byproducts of the fermentations and the performance of the catalytic oxidation of ethanol at metal catalysts in batch mode. This study examines the effects of multiple components such as ionic strength, cation size, buffering strength, alcohol concentration, fermentation/fuel cell byproducts, and interfering organics on fuel cell operation.

Published by Elsevier B.V.

1. Introduction

Due to energy demands and environmental concerns there has been a great interest in searching out renewable energy sources as an alternative to fossil hydrocarbons. These must also be environmentally sustainable and convenient to implement. There have been decades of research and development in the area of proton exchange membrane (PEM) fuel cells to provide clean, quiet power generation [1–3]. However, the traditional renewable fuels for PEM fuel cells, hydrogen and methanol, have significant hazards of flammability and toxicity. These hazards impose additional logistics burdens, in addition to safety issues for the end user.

Glucose has been proposed as a renewable energy source for several reasons. It has an energy density of 16 MJ kg^{-1}, lower than ethanol (30 MJ kg^{-1}) or gasoline (47 MJ kg^{-1}), but still quite high [4]. Unlike more traditional fuels, however, glucose is completely safe, being non-flammable and non-toxic, making it easier to store and transport, especially in many areas of the world without a fuel pipeline infrastructure. Provided glucose is kept dry, it is entirely inert, subject neither to evaporation nor to decay. Glucose can be produced simply, in an environmentally sustainable manner, and in many areas of the world. In addition, glucose can be scavenged locally from native ecosystems or from waste streams, an important consideration for minimizing logistics.

While glucose has some significant advantages there are some significant challenges in how it should be best utilized. It is not compatible with traditional PEM fuel cell technologies. Two options commonly suggested for electrochemical power generation from glucose are enzymatic or microbial fuel cells.

* Corresponding author. Tel.: +1 301 391 0252; fax: +1 301 391 0310.
E-mail addresses: david.m.mackie.civ@mail.mil (D.M. Mackie), sanchao.liu.ctr@mail.mil (S. Liu), marcus.s.benyamin.ctr@mail.mil (M. Benyamin), rganguli@teledyne-si.com (R. Ganguli), james.j.sumner4.civ@mail.mil (J.J. Sumner).

0378-7753/$ – see front matter Published by Elsevier B.V.
http://dx.doi.org/10.1016/j.jpowsour.2013.01.077

Enzymatic fuel cells have shown promise, but complete oxidation of glucose is necessary to gain full advantage of its high energy density. This is only possible if a cascade of enzymes is designed, all of which need to be stable in the same operational environment. Designing these cascades is an active area of research [5] but if one enzyme in a cascade losses activity it cannot be easily replaced, thus eventually causing the fuel cell to fail.

Microbial fuel cells (MFCs) utilize micro-organisms' natural enzyme cascades for effectively extracting energy from glucose. The microbes automatically detect and replace any inactive enzymes. The coulombic efficiency of MFCs is high, reaching 65% [6]. Unfortunately MFCs suffer significantly from low power density. The problem is that whole microbes serve as the catalysts. This limits the scale of the electrode materials to single micron dimensions because, for the highest electron transfer efficiency, the microbes need to be in direct contact with the electrode surface. These systems are limited to power densities of single W m^{-2} [6,7]. Attempts to get around this limitation of MFCs by using soluble electron mediators (which in theory would relieve the microbes of the necessity for direct electrode contact) have so far failed due to diffusion limitations. The power densities are not increased by the orders of magnitude that are required, and many soluble electron mediators are toxic or have proven to be unstable [8].

There have been demonstrations in the literature of using bio-derived alcohols in direct alcohol fuel cells (DAFCs) [9–12]. Performance is good – very much what one would expect from a PEM fuel cell. However, to date this has been accomplished by producing the alcohol, purifying it, and then diluting it in purified water to run in the DAFC. In this process, not only the energy from the oxidation of the glucose to alcohol is lost but also the purification steps are energy intensive, causing further energy loss. For real-life applications these parasitic losses must be minimized, yet in analyses of DAFC efficiency they are often overlooked. In a review of the literature, certain aspects of DAFCs have been explored in depth, such as the effects of utilizing ethanol as opposed to methanol [11–13], but parasitic loss has been mostly ignored.

Here we describe the use of a bio-hybrid fuel cell where the starting fuel, glucose, is oxidized to ethanol and parasitic power losses are limited by using the fermented ethanol in the DAFC with minimal preparation. The fuel cells described here are also passive: no liquids or gases are pumped past either electrode, no chemicals are added to facilitate the process, and (except for fermentations) they are run on the laboratory benchtop. To limit the scope, we first perform batch fermentation of glucose to ethanol with yeast (a well-studied process), then operate a DAFC in batch mode using the product of the fermentation. The only purification step is to filter out solids. Moving from using dilute alcohol in deionized water to the complex matrices of fermented media raises many questions about the performance and lifetime of the fuel cell and its components. These questions include but are not limited to the starting materials and byproducts of the fermentations, and the performance of the catalytic oxidation of ethanol at metal catalysts in batch mode. Some of these components include the glucose feedstock and the known oxidation products acetaldehyde and acetate [10]. While this would be sufficient for chemically derived fuels, to support yeast fermentations the organisms need other essential components in order to thrive. Therefore, this study also examines the effects of multiple other components such as ionic strength, cation size, buffering strength, alcohol concentration, fermentation/fuel cell byproducts, and interfering organics in the microbial media's composition (i.e. salts, amino acids, protein concentration, etc.). It should also be kept in mind that conditions suitable for fermentation are not ideal for PEM fuel cell operation [9].

2. Experimental materials and methods

2.1. Chemicals

Control experiments are conducted in either deionized (DI) water or a yeast growth medium, both with a known amount of ethanol (molecular biology grade, absolute, Sigma–Aldrich) added. All DI water used in this study is from a deionized reverse osmosis source passed through a Barstead Nanopure water polisher. Similarly, the acetaldehyde, sodium acetate, acetic acid, glucose, KH_2PO_4, Na_2HPO_4, NaCl, $MgSO_4$, and KCl are research grade or better, and are obtained from Sigma–Aldrich or Fisher.

Yeast (Bakers' Yeast, *Saccharomyces cerevisiae Type II*, Sigma) fermentations use D-(+)-Glucose from Sigma Life Science (SigmaUltra, 99.5%). Sterile filters (0.2 μm nylon) used to remove organisms and solids from the fermented media are from various manufacturers. Yeast nitrogen base (YNB) growth medium is from Difco prepared as directed for 1× solution, with 4% glucose added, then sterile-filtered. M9 growth medium is prepared as follows: 3 g KH_2PO_4, 6 g Na_2HPO_4 (anhydrous), 5 g NaCl, and 1 mL of 1 M $MgSO_4$ (120.37 g) are dissolved in DI water to make 1 liter (L) of solution, and sterile-filtered.

The chloride salts used to determine sensitivity of the DAFC to cation size are LiCl (Fisher Scientific Co.), CsCl (Alfa Aesar, 99.9%), and KCl and NaCl (Sigma). The 5% v/v sulfuric acid (H_2SO_4) used to clean the DAFC between runs is prepared from 50% v/v stock (Fluka) and DI water.

2.2. Supplies and instruments

The DAFCs are purchased from fuelcellstore.com (SKU 1071041, H-Tec Ind., GmbH, single plate methanol/air PEMFC), and are intended by the manufacturer as direct methanol fuel cells. The current collectors are stainless steel mesh. These fuel cells were selected to be similar to those used in bio-hydrogen generation studies [14–16].

For electrical measurements (current vs. time and linear sweep voltammetry) we use an Electrochemical Workstation from CH Instruments (Austin, TX), either the 660A model with a single-potentiostat or the 760B model with a bi-potentiostat. High-performance liquid chromatography (HPLC) measurements are performed with an Agilent HPLC 1200 equipped with a refractive index detector. The HPLC column is an Aminex HPX-87H cation exchange column (300 mm × 7.8 mm i.d.; 9 μm polystyrene divinylbenzene beads) from Bio-Rad Laboratories.

2.3. Experimental procedures

In order to differentiate between the effects of media components and fermentation products on DAFC performance, the investigation is performed in three stages. In the initial stage, the performance of the DAFCs with aqueous ethanol is carefully evaluated to establish a baseline for comparison. In the second stage, media is prepared with 3% (v/v) ethanol, to fuel the DAFCs. In the third stage, media containing 4% (w/v) glucose is prepared, and fermented to completion with yeast (4 days at 40 °C). The fermentate is sterile-filtered, with no other processing, and fuels the DAFCs. The DAFC performance is evaluated via amperometric (current vs. time, I–t) curves poised at 200 mV (for 1800 s, unless otherwise stated), followed by linear sweep voltammetry (LSV) from 0 to 600 mV at a scan rate of 1 mV s^{-1}. The DAFC's cathode is utilized both as a pseudo-reference and as the counter electrode for the LSV and amperometric current vs. time (I–t) experiments, as is common practice in PEM fuel cell analysis.

Obtaining repeatable electrochemical measurements on the DAFC requires proper conditioning and storage of the DAFC [17]. While stored, the DAFC is filled with 5% sulfuric acid solution. The openings for filling the anode compartment, as well as the vents for the cathode, are covered to reduce evaporation. Before data is collected, the DAFC is rinsed thoroughly with DI water, followed by preconditioning via an 1800 s amperometric protocol and another thorough rinse with DI water. If the performance with 3% ethanol in DI water as the fuel does not match the established baseline, then repeated preconditioning I–t runs are performed until consistent baseline performance is obtained.

The DAFC is cleaned after every run as recommended by the manufacturer. The recommended 1% (v/v) sulfuric acid requires impractically long soak times. However, soaking in 5% (v/v) sulfuric acid for 10–30 min restores the DAFC to normal function, even after operation with fermentates. Heavy-cation chloride salts are an exception and require repeated soaks in DI water followed by 30 min in 5% (v/v) sulfuric acid and subsequent rinses with DI water.

Samples are analyzed with HPLC to determine the identity and concentration of compounds present. This is done to evaluate both the fermentates and the byproducts from the operation of the DAFCs. The sample (5 μL) is injected into the system, eluted isocratically with a mobile phase of 3.25 mM sulfuric acid at 0.6 mL min^{-1} and 30 °C [18]. Quantification is based on an external calibration curve using pure components of known concentrations as standards. Stock solutions of 1, 2.5, 5, 10, 25, 50, 100, 250, and 500 mM were utilized. Calibration curves were generated by triplicate injections of each calibrator.

3. Results and discussion

First the performance of the DAFCs is carefully evaluated with aqueous ethanol to determine proper operating procedures and parameters, and to establish a baseline standard for comparison. Fig. 1 shows nine power curves derived from LSVs that are taken every 10 min up to 90 min. This is done in batch mode, where the DAFC is filled with 3% aqueous ethanol at 0 min and not refreshed throughout the duration. There are significant drops in power between the first several measurements that indicates the rapid change in current generation. For the run shown in Fig. 1, the current is still building during the early stages of the first measurement, as can be seen in the first 200 s of some current traces in Fig. 2. Therefore peak-power changes in Fig. 1 are not as dramatic as they could be. On the other hand, it is difficult to depict "typical" power curves. Although the monotonic fall-off in power is a recurring feature, the shapes of the first few LSVs are not readily predictable. These dramatic drops in power can be explained by the fact that some of the current generated is from double layer charging throughout the complex surface of the MEA in the first few minutes followed by a slow drop to steady state currents of the fuel cell operation. This occurs every time the fuel cell is cleaned extensively. Emptying and refilling the anode compartment lessens the effects, especially in the first few minutes, but it was determined that it took approximately 20 min to reach steady state.

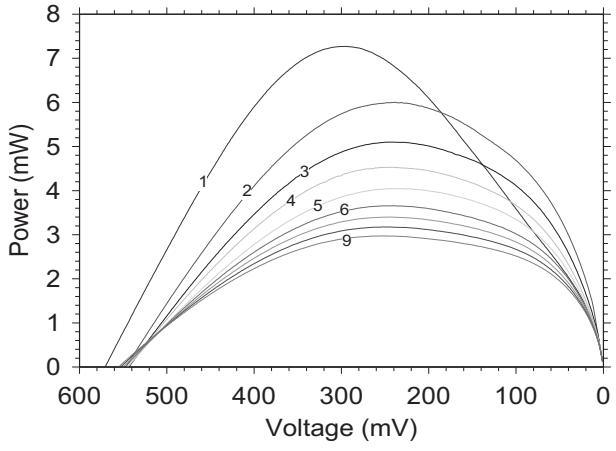

Fig. 1. Power curves plotted from LSVs collected in batch mode on a DAFC using 3% (v/v) aqueous ethanol. The fuel cell is filled at $t = 0$ and LSVs are collected at 10 min intervals from 0 to 600 mV at a scan rate of 1 mV s^{-1}. This shows dramatic changes in operation over the first several scans, and peak power decreasing monotonically.

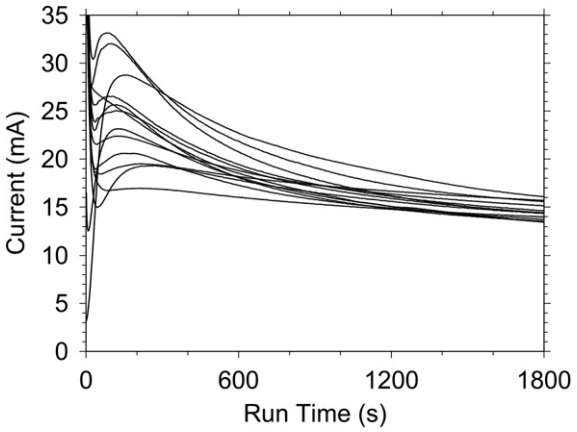

Fig. 2. Examples of I versus t traces under a 200 mV bias for a DAFC with 3% (v/v) aqueous ethanol as the fuel. Note that the first 10 min have significant scatter but that after 30 min the results are much more reproducible.

Fig. 2 is complementary to Fig. 1 and shows examples of amperometric current vs. time (I–t) traces under a 200 mV bias for multiple experiments using a DAFC with 3% aqueous ethanol as the fuel. Not only are changes during runs dramatic during the first 15 min, but also there is great variability from run to run, depending upon starting conditions and the DAFC's recent history. However, it isn't necessary to wait very long for good repeatable data. Over time the run-to-run variation settles, and runs become fairly standard by 30 min.

Also note from Fig. 1 that the peak power occurs at about 200 mV, so that voltage is selected as the poised potential for I–t experiments. Throughout the rest of the experiments, each I–t measurement is allowed to proceed for a set time of 30 min (1800 s). Also, unless otherwise stated, preconditioning via the half-hour I–t protocol is conducted before collecting LSVs. Doing so greatly improves the reproducibility of the results. Whenever possible, DAFC I–t and LSV results are compared against those for a standard run, which is selected to be 3% (v/v) ethanol in DI water (EtOH 3% aq).

Fuel cell performance is concentration dependent, and Fig. 3 shows why we choose 3% ethanol as our standard. (Compare Zhao et al. [1] for methanol DAFCs.) Concentrations of 0.15, 0.3, 1.0, 1.5, 2.0, 3.0, 4.0, 5.0, 6.0% (26, 52, 170, 260, 340, 520, 690, 860, 1000 mM) ethanol are shown. The current data (circles, left axis) are from I–t measurements. The peak power data (triangles, right axis) are from power curves derived from the LSV measurements immediately following each I–t measurement. Note that the peak power for each ethanol concentration is not necessarily at 200 mV, and that the active area of the membrane electrode assembly (MEA) is 2.68 cm^2. Choosing 4% ethanol as a standard would give slightly higher performance, but the flatness of the curve at that percentage would cause difficulties in evaluating the performance of fermented media. (The effect of imperfect fermentations, which result in lower than ideal ethanol percentages, would be obscured.)

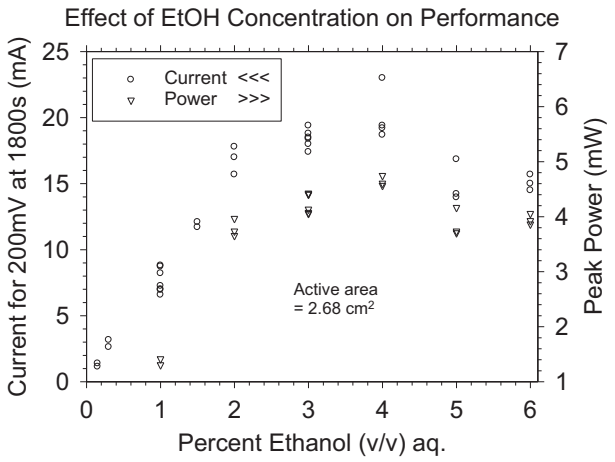

Fig. 3. Plot of the current generated (circles, left axis) via *I*–*t* measurements at a poised potential of 200 mV and the peak power (triangles, right axis) from power curves derived from the LSV measurements, 0–600 mV sweep at a scan rate of 1 mV s^{-1}, immediately following each *I*–*t* measurement. Concentrations of 0.15, 0.3, 1.0, 1.5, 2.0, 3.0, 4.0, 5.0, 6.0% (26, 52, 170, 260, 340, 520, 690, 860, 1000 mM) ethanol are shown. Note that the peak power for each ethanol percentage is not necessarily at 200 mV, and that the active area of the MEA is 2.68 cm^2.

In the second stage, the effects of microbial media on the operation of a DAFC are studied. Two common yeast fermentation media, M9 and YNB, are "spiked" with 3% (v/v) ethanol, and used to fuel the DAFC. As a control, performance is compared to deionized water (DI), "spiked" with 3% (v/v) EtOH. M9 is a minimal medium which has high salt concentration and high buffering capacity, but does not add any excess organics which are potential interferents. YNB is a more complex medium with amino acids, vitamins, and minerals added for microorganisms' health; however, it has a lower ionic strength and buffering capacity than M9. DI, of course, has no interferents, ionic strength, or buffering capacity. Fig. 4 compares the performance of the three fuels. Part a) shows *I*–*t* plots, at a poised potential of 200 mV. Part b) shows the LSV measurements taken immediately after the corresponding *I*–*t* measurements, and the derived power curves. Note that the performance of the YNB-based fuel is comparable to that of the DI-based fuel, while that of the M9-based fuel lies significantly below the other two. For YNB, peak power is lower by 24%, and M9's is lower by 60%.

To our knowledge, the effect of varying salt composition and concentration in the fuel supply is an unexplored issue for DAFCs. There are three main factors that should be considered when examining the effect of salts on fuel cell performance: cation size, buffer capacity, and ionic strength. The effect of cation size is examined by using chloride salts of Li, Na, K, Cs at the same cationic molarity as the M9 medium (194 mM) with 3% (v/v) ethanol in DI. Buffering is also fixed, since the chloride salts all have negligible buffering capacity. Fig. 5 shows *I*–*t* curves (200 mV bias) for these four fuels, each one separately normalized by a preceding standard run with EtOH 3% aq. The most important point is that performance at 1800 s is low in all cases, ranging from 40% of the standard to only 14%. Clearly, cations commonly found in yeast fermentation media are harmful to DAFC performance. (In making this series of measurements, an unusually large amount of rinsing with DI and soaking in sulfuric acid is necessary to maintain the performance of the standard runs.) Also, the data is scattered, with no trend. It was thought that the larger cations would be more likely to slow diffusion in the PEM and therefore give worse performance, but any such effect seems not to be significant under these conditions.

The main component of M9 is phosphate buffered saline, which has a very high buffer capacity. This would essentially control the pH to near neutral in M9. YNB is also buffered, but with only one-

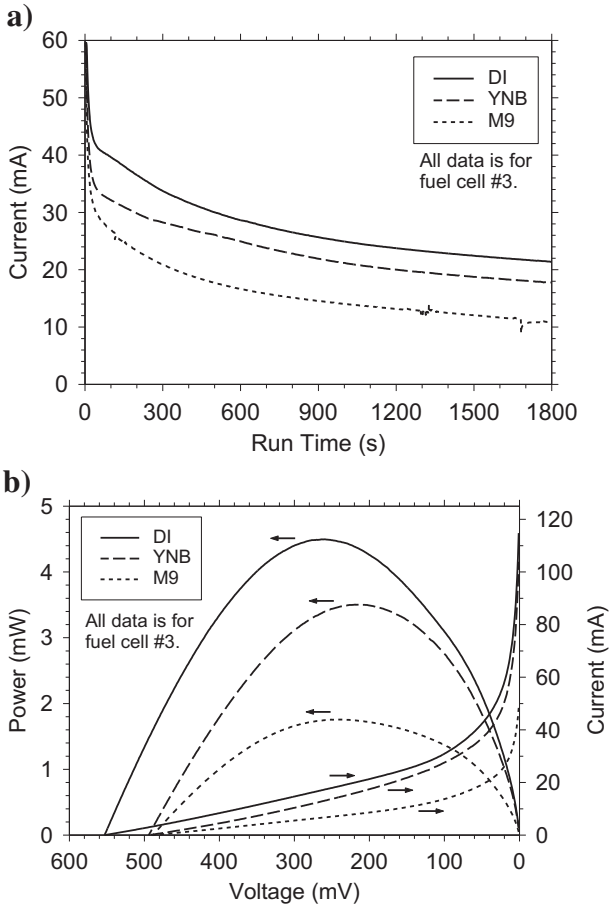

Fig. 4. Performance of batch DAFC for 3% (v/v) ethanol solutions of DI water and two types of fermentation media (M9 and YNB). Part a) shows *I*–*t* plots, at a poised potential of 200 mV. Part b) shows the LSV measurements taken immediately after the corresponding *I*–*t* measurements, and the derived power curves.

ninth the capacity of M9, while the pure aqueous and the alkali-metal/chloride solutions have essentially no buffering capacity. Through all of the experiments in this work, water and YNB solutions of ethanol always outperform M9. That fact would lead one to

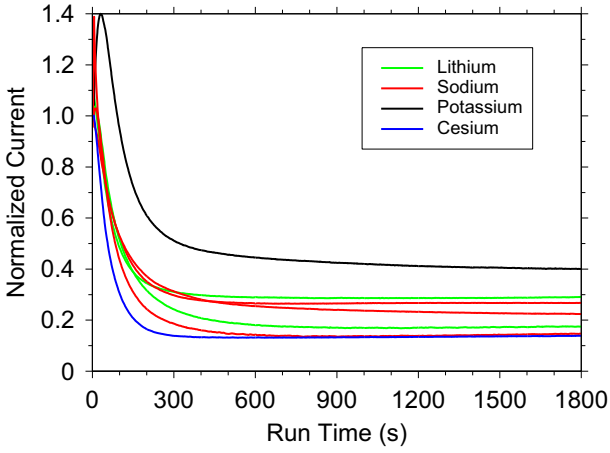

Fig. 5. Plot of the *I* vs. *t* curves (200 mV bias) generated with aqueous, 3% (v/v) ethanol solutions with the addition of chloride salts of Li, Na, K, Cs at the same molarity as the M9 medium (194 mM). Each current is separately normalized to a preceding baseline of 3% (v/v) ethanol in water with no salt added. The repeat green and red traces show replicates of the Li and Na salts.

conclude that the buffering could be playing a role. The main end product of ethanol break-down by most DAFCs is acetic acid. Without buffering, acetic acid would lower the pH, and the PEM performance should increase, explaining the improved performance for YNB and aqueous solutions. However, the alkali-metal/chloride solutions do no better (or worse) than M9, which would lead one to conclude that buffering is not playing a major role.

The effect of the concentration of ionic species is demonstrated in Fig. 6, which shows normalized *I*–*t* current at 1800 s for various concentrations of "spiked" M9. Neat (100%) M9 is diluted with DI water to reduce the ionic strength, then "spiked" to a concentration of 3% (v/v) ethanol. Although diluting the M9 also reduces its buffering capacity, even 25% M9 still has significant buffering capacity, considering the small amount of acetic acid produced over 30 min. Therefore, practically speaking, buffering is roughly constant for the M9 data (open circles) in Fig. 6 (except for the 0% data point). Clearly, DAFC performance is strongly influenced by anion concentration. That explains most of the performance decrease of "spiked" M9 compared to "spiked" YNB, since M9 has a higher ionic molarity. However, also shown in Fig. 6 is a filled square indicating the performance of "spiked" YNB plotted at the M9 percentage with the equivalent ionic molarity. (This square is actually 3 replicate data points grouped closely together.) At that ionic molarity, there still appears to be a small positive benefit for reduced buffering capacity. On the other hand, NaCl and KCl solutions with no buffering capacity don't outperform M9 at equivalent salt concentrations because the ionic molarity of all three solutions is so high that it overwhelms the buffering effect. Also a high ionic molarity increases the difficulty of obtaining reproducible results. This is opposite to what has been reported in the literature for traditional biofuel cells such as microbial systems where increasing ionic molarity has helped performance [19]. However this increase in performance is in cases where the electron transfer to the anode is due to microbes rather than oxidation at a metal catalyst.

In overnight data collections of *I*–*t* plots, the current decrease appears to match fuel utilization rates. While the media components affect the maximum sustained currents generated, they only slightly affect the long-term byproducts of the oxidation at the fuel cell anode. The literature indicates that in flowing systems the oxidation of ethanol at PtRu catalysts usually yields 55% acetaldehyde, 44% acetic acid and 1% carbon dioxide [13] while platinum alloys such as Pt/Sn, operated at increased temperatures, can yield up to 30% carbon dioxide [10].

Fig. 7 shows the progression of 3% (v/v) ethanol oxidation in batch operated DAFCs. Panels a) and b) are for DI water; c) and d) are for M9. Panels a) and c) show chromatograms of the fuel from DAFCs operating for the indicated time. Panels b) and d) display the concentrations of ethanol, acetic acid, and acetaldehyde as functions of reaction (operating) time. Note that the ethanol utilization and acetaldehyde/acetic acid production in the fuel cell with M9 [panels c) and d)] are slightly impeded, possibly due to the lower currents, indicating slowed kinetics. In the batch experiments run overnight, HPLC is used to track the concentrations of ethanol, acetaldehyde, and acetic acid. Ethanol is almost completely consumed (initial concentrations of 510 mM are reduced to 3.4 mM), there is no detectable acetaldehyde, and about 55% of ethanol is converted to acetic acid (ending concentration of 280 mM). The remaining carbon is either oxidized to carbon dioxide, or else is lost due to acetaldehyde evaporation. Simple modeling (not shown here) indicates the latter is likely. In flowing systems there is possibly not enough residence time in the anode for acetaldehyde to undergo the next step and be oxidized to acetic acid. The main differences between samples prepared in DI water versus M9 are the acetaldehyde produced in short-time samples (1–2 h), the steepness of the ethanol and acetic acid curves, and the total amounts of acetic acid produced throughout a run. Samples prepared in M9 show significantly less acetaldehyde than samples prepared from DI water. This lower concentration of acetaldehyde early in the experiments makes sense as the lower currents produced in fuel cells containing M9 indicate slower consumption of the ethanol fuel.

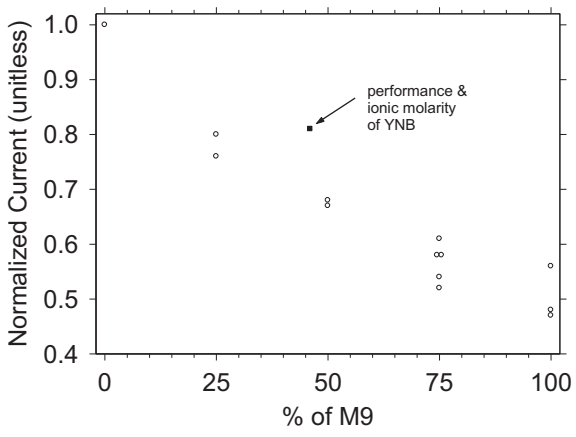

Fig. 6. Normalized current at 1800 s for aqueous M9 spiked with 3% (v/v) ethanol. Prior to spiking, neat (100%) M9 was diluted with DI to change the ionic strength. Note that the performance is significantly influenced by the salt concentration.

Acetaldehyde concentration builds at the beginning of the fuel cell operation and then drops off, but the concentrations remain low (single mM) through the run until dropping to essentially zero. One important reason is that the acetaldehyde can be oxidized by the DAFC anode, as shown in Fig. 8. Currents generated by the oxidation of acetaldehyde are significantly lower than that of ethanol throughout the run, but are not negligible. If the acetaldehyde current is multiplied by 2, to account for the fact that ethanol oxidation to acetic acid is a 4 electron process while acetaldehyde oxidation to acetic acid is only a 2 electron process, then these curves overlap reasonably well. The acetaldehyde curve drops faster, which could simply be due to faster evaporation as compared to ethanol. However, clearly the overall rate constant is not significantly different.

In extended runs acetaldehyde may also be lost due to evaporation as evidenced in Table 1. Table 1 indicates multiple things about DAFC operation with acetaldehyde present. Acetaldehyde as received contained approximately 10% acetic acid, possibly due to oxidation while in storage. Also, for DAFCs operating on acetaldehyde solutions about 50% either evaporates or is oxidized to carbon dioxide, while for DAFCs left at open circuit about 70% either evaporates or is oxidized. The results from this table for ethanol solutions operated in DAFCs for 14 h can be compared to the results from different runs reported in Fig. 7. The acetic acid and ethanol concentrations match equivalent time points in Fig. 7. Operation on ethanol shows that about 30% either evaporates or is oxidized to carbon dioxide, which matches Fig. 7 at 15 h. This is consistent with Lamy et al. [10] which reports 30% of the total carbon in ethanol oxidizes directly to carbon dioxide, a 12-electron process, at Pt alloy catalysts. Some more exotic catalysts can oxidize the ethanol predominantly to CO_2 [12,20]. In general, acetic acid is not consumed at the anode (like acetone and glucose), and does not readily evaporate since it has a significantly lower vapor pressure. Unfermented glucose shows little to no current generation in a DAFC. Acetic acid and sodium acetate solutions prepared along with DI water controls show no current generation at all.

In the final stage of this investigation, prepared ethanol fuel and fermented media are directly compared. Results are shown in Fig. 9 which includes LSVs and power curves for fuel cells operated with

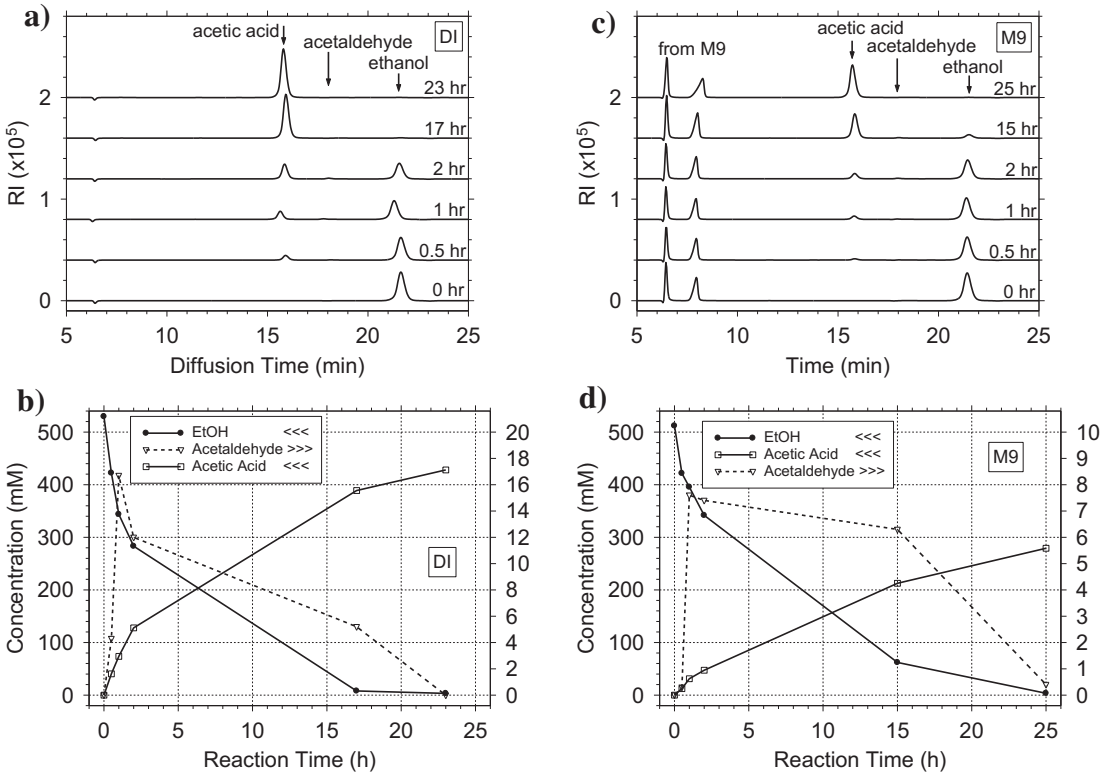

Fig. 7. Progression of 3% (v/v) ethanol oxidation in batch operated DAFCs. Panels a) and b) are for DI water; c) and d) are for M9. Panels a) and c) show chromatograms of the fuel from DAFCs operating for the indicated time. Panels b) and d) display the concentrations of ethanol, acetic acid, and acetaldehyde as functions of reaction (operating) time. Note that the ethanol utilization and acetaldehyde/acetic acid production in the fuel cell with M9 [panels c) and d)] are slightly impeded, possibly due to the lower currents, indicating slowed kinetics.

1) 3% ethanol in DI water, 2) fermented YNB, or 3) fermented M9. Both media solutions are started with 4% glucose; however, the M9 minimal media have more yeast added.

A typical fermentation of 4% glucose by yeast would yield approximately 3% ethanol. These data plots show that the YNB fermentation produces about 35% less power as compared to the DI water control while the M9 system is significantly (79%) lower. For direct comparison of raw fuel cell performance refer to the results with spiked media, Fig. 4. The results are similar; however the YNB has slightly reduced and M9 has significantly reduced performance. Note that sterile filtration through a 0.22 micron filter was the only sample processing conducted. There was no other purification, separation, or concentration of the bio-ethanol and nothing was added to the fermented fuel.

From the information presented it may be surmised that these performance reductions could be explained primarily by ethanol concentration and ionic strength. Ethanol concentration of the media, fermented for four days then filtered, is measured via HPLC. The DI water samples are prepared with 515 mM ethanol (3%). YNB fermentations produce 410 mM (~2.4%) ethanol. Using the same amount of starting yeast, fermentations with M9 produce only 32 mM (~0.2%). However, when starting with about twenty times as much yeast, M9 yields 360 mM (2.0%) ethanol. Referring back to Fig. 3, typical power output from a fuel cell with 3% ethanol in DI water is ~4.2 mW (100% power). In comparison, aqueous ethanol

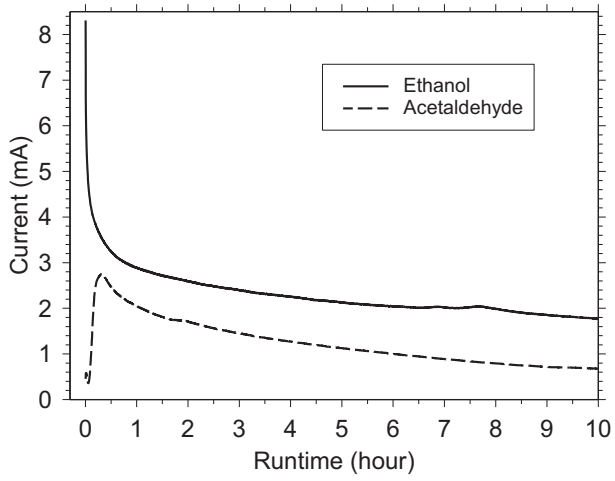

Fig. 8. Plot of the *I* vs. *t* curves (200 mV bias) generated with 3% (v/v) ethanol and acetaldehyde in M9. Note that the currents generated by the oxidation of acetaldehyde are significantly lower than those of ethanol throughout the run.

Table 1
Concentrations of acetic acid, acetaldehyde, and ethanol determined by HPLC. Data identified as *sit* are generated from fuel cells not connected to a load. Those identified as *run* are operated under the amperometric (*I* vs. *t*) protocols at a bias of 200 mV. This verifies that no acetaldehyde is present at $t = 0$ or $t = 14$ h for fuel cells prepared with 3% ethanol but samples prepared with 3% acetaldehyde do leave trace amounts whether being operated or stored.

(Units = mM)	Acetic acid	Acetaldehyde	Ethanol
Fuel = 3% (v/v) acetaldehyde in DI water			
0 h, control	59	439	0
12 h, run (sit)	260 (173)	11 (33)	0 (0)
Fuel = 3% (v/v) ethanol in DI water			
0 h, control	0	0	565
14 h, run (sit)	404 (196)	0 (0)	11 (54)

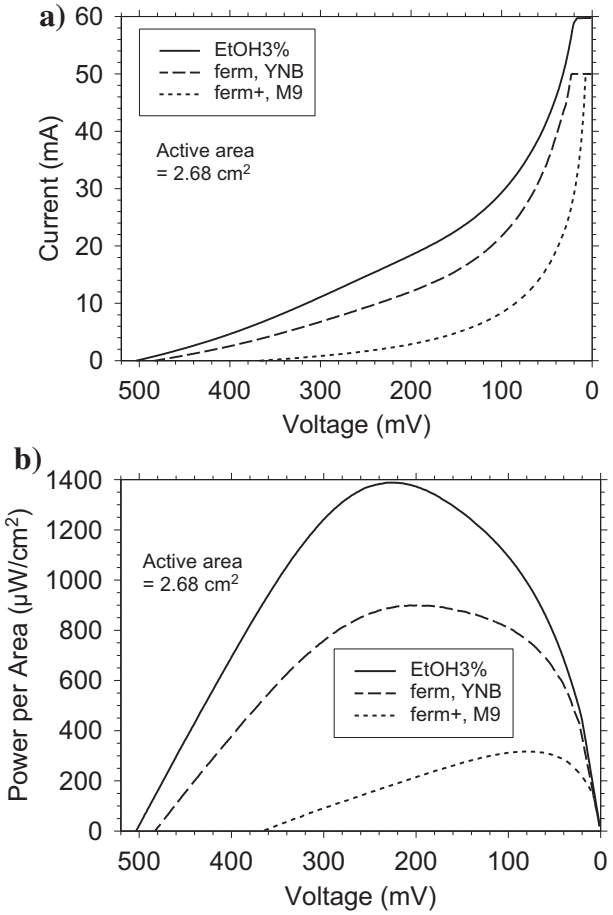

Fig. 9. Performance of DAFC for fermented media and control. Part a) shows LSV measurements, 0–600 mV sweep at a scan rate of 1 mV s^{-1}, each immediately following an *I–t* measurement (poised at 200 mV) for 1800 s. Part b) shows the power curves derived from the LSV measurements, plotted as power per unit area. The DAFC is filled with fermented YNB filtrate, fermented M9 filtrate, or 3% (v/v) ethanol in DI water as a control. Fermentations are run for 4 days at 40 °C, starting with 4% (w/v) glucose and bakers' yeast (*S. cerevisiae*).

at a concentration equal to the YNB fermentate's would produce ~3.8 mW (90% power), significantly more than the 65% power shown in Fig. 9. Moreover, aqueous ethanol at a concentration equal to the best M9 fermentate's would produce ~3.5 mW (83% power), much more than the 21% power shown in Fig. 9 (and at a higher voltage).

The degraded performance with increasing ionic strength (salt concentration) is needed to explain these further reductions in peak power. Referring back to Figs. 4 and 6, "spiked" YNB produces 80% of the power produced by "spiked" DI water samples. Multiplying this 80% by the 90% power produced with the reduced ethanol concentration yields 70%, in good agreement with the 65% result from Fig. 9. M9 suffers a penalty of about 50% from ionic strength. Multiplying 50% (power from the increased ionic strength) by 83% (power from the decreased ethanol concentration) yields 40%, twice the result from Fig. 9. This even lower performance may be due to adding 20 times more yeast to the fermentation, which changes the medium significantly.

4. Conclusions

This is the first report to show the feasibility of using fermented sugars in a DAFC with only filtration as sample preparation. These results show good potential for using fermented microbial media directly with only a simple filtration step to remove cellular mass from the complex mixture before use. The work presented here shows that some media compositions when fueled with the same concentration of ethanol have very comparable performance to samples prepared with DI water and a variety of factors were examined concerning the performance of DAFCs.

It was determined that measurement technique, time, and fuel cell preparation are critical to obtaining reproducible results. It was verified that ethanol concentration is a major influence on the performance of a DAFC. However the composition of the media used in the fermentation of sugar to ethanol also plays a major role. The main factor influencing DAFC performance is the ionic strength of the medium. Higher salt concentrations result in significantly lower peak powers from the fuel cells (in contrast to microbial fuel cells). Buffer capacity, cation size, and presence of additional organics (including residual glucose) play a lesser role.

Future work would include determining media compositions optimized for the combination of fuel cell performance and effective fermentation. Also, long term performance of fuel cell operation and the effect of environmental conditions need to be explored. While the performance can suffer due to operation on fermentate, this can be minimized. It should also be considered that a sugar fuel source is not only renewable but also non-flammable, non-toxic, and has the potential to be scavenged from saps, food wastes, or waste waters. These indigenous sources could be fermented and then used directly in the fuel cell. This would reduce the logistics load required in deploying conventional PEM fuel cell technology, and eliminate the hazards of transporting and manipulating fuels such as hydrogen or methanol. The only necessary pretreatment of the fermentates would be filtering insoluble cellular mass from the fuel.

Acknowledgments

The authors acknowledge funding from the U.S. Army's Institute of Collaborative Biotechnologies (ICB) under contract number W911NF-09-D-0001. The authors also acknowledge K. Chu for laboratory support and D. Chu for helpful conversations as well as the support of the US Army Research Laboratory, Sensors and Electron Devices Directorate (ARL-SEDD). M.B. acknowledges the Science and Engineering Apprenticeship Program (SEAP) for support. S.L. acknowledges General Technical Services (GTS) for administrative support.

References

[1] T.S. Zhao, R. Chen, W.W. Yang, C. Xu, Journal of Power Sources 191 (2009) 185–202.
[2] X. Cheng, Z. Shi, N. Glass, J.J. Zhang, D.T. Song, Z.S. Liu, H.J. Wang, J. Shen, Journal of Power Sources 165 (2007) 739–756.
[3] N. Lymberopoulos, Fuel Cells and Their Application in Bio-energy, Report Center for Renewable Energy Sources (CRES), European Commission DG-TREN, 2005, Contract number NNE5-PTA-2002-003/1.
[4] P.W. Atkins, The Elements of Physical Chemistry, Oxford University Press, Oxford, 1993, p. 70, (Calculated from the standard enthalpies of combustion.).
[5] D. Sokic-Lazic, R.L. Arechederra, B.L. Treu, S.D. Minteer, Electroanalysis 22 (2010) 757–764.
[6] B.E. Logan, Microbial Fuel Cells, John Wiley and Sons, Hoboken, NJ, 2008.
[7] M.H. Zhou, H.H. He, T. Jin, H.Y. Wang, Journal of Power Sources 214 (2012) 216–219.
[8] H.E. Xie, E.L. Li, Z.K. Tang, Journal of Chemical Technology and Biotechnology 86 (2011) 109–114.
[9] T. Tsujiguchi, T. Furukawa, N. Nakagawa, Journal of Power Sources 196 (2011) 9339–9345.
[10] C. Lamy, E.M. Belgsir, J.M. Leger, Journal of Applied Electrochemistry 31 (2001) 799–809.
[11] W.J. Zhou, B. Zhou, W.Z. Li, Z.H. Zhou, S.Q. Song, Q. Xin, S. Douvartzides, M. Goula, P. Tsiakaras, Journal of Power Sources 126 (2004) 16–22.

[12] J. Barroso, A.R. Pierna, T.C. Blanco, J.J. del Val, Physica Status Solidi A 208 (2011) 2309–2312.
[13] H. Wang, Z. Jusys, R.J. Behm, Journal of Power Sources 154 (2006) 351–359.
[14] S. Oncel, F. Vardar-Sukan, Journal of Power Sources 196 (2011) 46–53.
[15] D. He, Y. Butel, J.P. Magnin, C. Roux, J.C. Willison, Journal of Power Sources 141 (2005) 19–23.
[16] R. Wunschiers, P. Linblad, International Journal of Hydrogen Energy 27 (2002) 1131–1140.
[17] X.Z. Yuan, S.S. Zhang, J.C. Sun, H.J. Wang, Journal of Power Sources 196 (2011) 9097–9106.
[18] G.C. Ehrlich, D.F. Goerlitz, J.H. Bourell, G.V. Eisen, E.M. Godsy, Applied and Environmental Microbiology 42 (1981) 878–885.
[19] H. Liu, S.A. Cheng, B.E. Logan, Environmental Science & Technology 39 (2005) 5488–5493.
[20] A. Kowal, M. Li, M. Shao, K. Sasaki, M.B. Vukmirovic, J. Zhang, N.S. Marinkovic, P. Liu, A.I. Frenkel, R.R. Adzic, Nature Materials 8 (2009) 325–330.